Chinese Chemical Letters 34 (2023) 107236

Contents lists available at ScienceDirect

Chinese Chemical Letters

journal homepage: www.elsevier.com/locate/cclet

Biomass derived Fe-N/C catalyst for efficiently catalyzing oxygen reduction reaction in both alkaline and neutral pH conditions

Lin-Qian Yu, Hao Wang, Shu-La Chen, Te-Er Wen, Bao-Cheng Huang*, Ren-Cun Jin

Laboratory of Water Pollution Remediation, School of Life and Environmental Sciences, Hangzhou Normal University, Hangzhou 311121, China

ARTICLE INFO

Article history:
Received 16 December 2021
Revised 18 January 2022
Accepted 15 February 2022
Available online 19 February 2022

Keywords:
Fe-N/C
Oxygen reduction reaction
Biomass
Fe coordination
Polyphenol

ABSTRACT

Fe-N/C is a promising oxygen reduction reaction (ORR) catalyst to substitute the current widely used precious metal platinum. Cost-effectively fabricating the Fe-N/C material with high catalytic activity and getting in-depth insight into the responsible catalytic site are of great significance. In this work, we proposed to use biomass, tea leaves waste, as the precursor to prepare ORR catalyst. By adding 5% $FeCl_3$ (wt%) into tea precursor, the pyrolysis product (*i.e.*, 5%Fe-N/C) exhibited an excellent four-electron ORR activity, whose onset potential was only 10 mV lower than that of commercial Pt/C. The limiting current density of 5%Fe-N/C (5.75 mA/cm^2) was even higher than Pt/C (5.44 mA/cm^2). Compared with other biomass or metal organic frameworks derived catalysts, 5%Fe-N/C showed similar ORR activity. Also, both the methanol tolerance and material stability performances of as-prepared 5%Fe-N/C catalyst were superior to that of Pt/C. X-ray adsorption fine structure characterization revealed that the FeN_4O_2 might be the possible catalytic site. An appropriate amount of iron chloride addition not only facilitated catalytic site formation, but also enhanced material conductivity and reaction kinetics. The results of this work may be useful for the Fe based transition metal ORR catalyst design and application.

Fuel cell technology is one of the favorable solutions for sustainable transportation development. Nevertheless, the low rate of oxygen reduction reaction (ORR) on cathode surface remains as a great challenge for its application [1–3]. Due to its low Fermi level [4], platinum-based catalysts usually exhibit excellent ORR activity, yet the low storage reserves and fancy price impeded its large-scale and sustainable deployment [5,6]. As platinum is short of supply, there is a considerable motive force to search for abundant and inexpensive materials to expand the development of fuel cell technology [7,8].

Transition metal-nitrogen-carbon electrocatalyst, especially Fe-N/C material, has been widely synthesized and used to catalyze ORR, by considering its high level in both activity and stability [8–10]. Although a substantial progress on selectivity improvement of four-electron reaction route has been achieved, the intrinsic catalytic site of Fe-N/C still remains elusive. Fe-N moiety (Fe-N_x) was identified as the primary active center for ORR, while the metal coordination environment change normally results in discrepant catalytic selectivity [11,12]. For instance, FeN_4 structure was widely proposed as the catalytic site in the previous works [13,14]. Whereas, other studies argued that five [15] or six [16] coordinated Fe-N_x was the responsible structure to catalyze ORR. Therefore, the responsible Fe-N_x site is still ambiguous. Under the actual situation, other elements such as oxygen or carbon are possible to involve in coordination [17]. Getting in-depth insight into the Fe-N/C catalyst active site identification and enrichment is then of great significance for ORR rate improvement and fuel cell application.

Metal-organic coordinates were favorable materials to prepare metal-N/C catalyst. Zeolitic imidazolate frameworks-8 was used to coordinate Fe by partial substitution of zinc ions [18]. Fe-N/C hybrid materials could also be fabricated *via* annealing Zn and Fe bimetallic metal organic frameworks (MOFs) [19]. However, most of previous studies utilized artificially synthesized organic frameworks as precursors to prepare Fe-N/C ORR catalysts.

While the preparation of MOFs is complicated, the reuse of waste biomass is much more convenient. There are a series application of waste biomass derived catalysts in photocatalysis [20], electrocatalytic water oxidation reaction [21], oxygen evolution [22,23], as well as ORR catalysis [24]. Notably, naturally accessed polyphenol structure was proposed as an outstanding candidate to lock metal ion [25]. Our previous work also showed that cobalt nanocomposite could be successfully fabricated by using tannic acid as organic ligand [26]. Herein, polyphenol substance might be used an efficient organic ligand to anchor iron ion for Fe-N/C

* Corresponding author.
E-mail address: huangbc@hznu.edu.cn (B.-C. Huang).

https://doi.org/10.1016/j.cclet.2022.02.041
1001-8417/

preparation. Typically, as one of the popular drink around the work [27], tea leaves are rich in polyphenol components. According to statistics, more than 90% of tea is left as waste in the tea beverage industry [28]. Therefore, the reuse of tea leaves waste is worthy of attention. Specifically, green tea extract acts as both reducing agent and capping agent in the synthesis of iron nanoparticles [29], which may benefit for the Fe dispersion.

Based on the above understandings, the primary aim of this work was to explore the feasibility of using waste tea leaves to prepare Fe-N_x enriched Fe-N/C ORR catalyst. A serial of catalysts were synthesized and their ORR performances under both alkaline and neutral pH conditions were tested. Then, the active catalytic site was identified *via* synchrotron radiation characterization. At last, the catalyst structure-function relationship was elucidated. The result of this work may be useful for the transition metal ORR catalyst development.

The schematic synthetic route of Fe-N/C catalyst was given in Text S1 (Supporting information). All of the electrochemical tests were conducted in a three electrode device through a CHI 760E workstation. Detailed parameters were listed in Text S2 (Supporting information). The characterization tests and parameters were provided in Text S3 (Supporting information).

Scanning electron microscopy (SEM) images show that 5%Fe-N/C owns fine granular form, while 7.5%Fe-N/C and 10%Fe-N/C possess larger granular form (Fig. S1 in Supporting information). The Brunauer-Emmett-Teller specific surface area tests (Fig. S2 in Supporting information) revealed that 0%Fe-N/C owned the highest surface area (695.6 m^2/g), while 5%Fe-N/C (485.3 m^2/g), 7.5%Fe-N/C (370.8 m^2/g), and 10%Fe-N/C (271.3 m^2/g) were relatively low (Table S2 in Supporting information). The I_D band (~1370 cm^{-1}) and I_G band (~1590 cm^{-1}) of Raman spectra represent the defect and graphitic carbon [30], and the value I_D/I_G can normally reflect the defect degree of materials. As shown in Fig. S3a (Supporting information), the I_D/I_G values of four catalysts were discrepant, indicating the different graphitization degree of catalysts. The addition of $FeCl_3$ had significant effect on the defects of tea derived carbon materials, specifically, 5% $FeCl_3$ addition of $FeCl_3$ increased the graphitization degree of catalysts, otherwise, 7.5% $FeCl_3$ and 10% $FeCl_3$ decreased it. The graphitization degree of catalysts could influence the conductivity of the material [31]. Therefore, it may cause the alteration of material resistance. The X-ray diffraction (XRD) patterns (Fig. S3b in Supporting information) showed that graphite (PDF #89–7213) was the main carbon crystal morphology, yet, the crystallinity is poor. Also, Fe_3O_4 (PDF #75–0033) and α-Fe_2O_3 (PDF #84–0306) were found in 5%Fe-N/C, 7.5%Fe-N/C and 10%Fe-N/C. Among them, the 5%Fe-N/C showed the highest Fe_3O_4 peak intensity, while the 10%Fe-N/C exhibited the strongest Fe_2O_3 signal. Previous study revealed that the surface graphitic layer may prevent the acid to act on the inner metals [32], which might be the reason of iron oxides existence after acid pickling.

To explore the distribution of surface elements, the scanning electron microscopy-energy dispersive spectrometer (SEM-EDS) elemental mappings were collected (Figs. S4-S6 in Supporting information). It can be observed that N, O, and Fe elements were evenly distributed within materials. Inductively coupled plasma spectrometer test result showed that the Fe content of three catalysts were similar, ranging at 1.7%−2.1% (Table S3 in Supporting information). To further explore the surface elemental structure characteristics, the X-ray photoelectron spectroscopy (XPS) survey spectra of catalysts were given in Fig. S7. The high resolution N 1s and Fe 2p XPS spectra were then collected and resolved. As shown in Fig. 1a, N 1s spectra of 0%Fe-N/C shows two peaks at 401 eV [8] and 399.9 eV, representing graphitic N and pyrrolic N [33]. For 5%Fe-N/C (Fig. 1b), there are four peaks in the N 1s spectra, *i.e.*, 398.4 eV [8], 399.1 eV [34], 399.9 eV and 401 eV. The peak at 399.1 eV may attribute to the Fe-N_x species, and other three peaks attribute to pyridinic N, pyrrolic N and graphitic N. In comparison, no Fe-N_x moiety was found on 7.5%Fe-N/C (Fig. 1c). The peaks found on 10%Fe-N/C was the same to that on 5%Fe-N/C (Fig. 1d) As summarized in Table S4 (Supporting information), adding $FeCl_3$ would effectively transform graphitic N into pyridinic N in catalysts. Fe 2p spectra proved that addition of $FeCl_3$ would result in Fe-species formation within the pyrolysis products (Figs. 1e-h). Specifically, two peaks at 711.1 eV and 724.5 eV, which were ascribed to Fe(III) in relation to the Fe-N_x species [35,36], were observed on catalysts. The above Fe species matched well with the N 1s XPS spectra.

The ORR activity of as-prepared catalysts was further evaluated via a rotating ring-disk electrode. The LSV curves in Fig. 2a clearly indicate that the catalyst without iron addition (0%Fe-N/C) exhibited a poor activity in 0.1 mol/L KOH electrolyte, whose limiting current was 4.57 mA/cm^2. Iron was found to be beneficial for the ORR activity improvement but over dosage of iron into precursor would result in a decreased performance. Among the catalysts, 5%Fe-N/C showed the highest ORR activity, whose onset potential (0.93 V), half-wave poetical (0.84 V), and limiting current (5.75 mA/cm^2) were all comparable to commercial 20% Pt/C (Table S5 in Supporting information). For electrochemical ORR, 2-electron reaction intermediate (*i.e.*, H_2O_2) formation is the main obstacle.

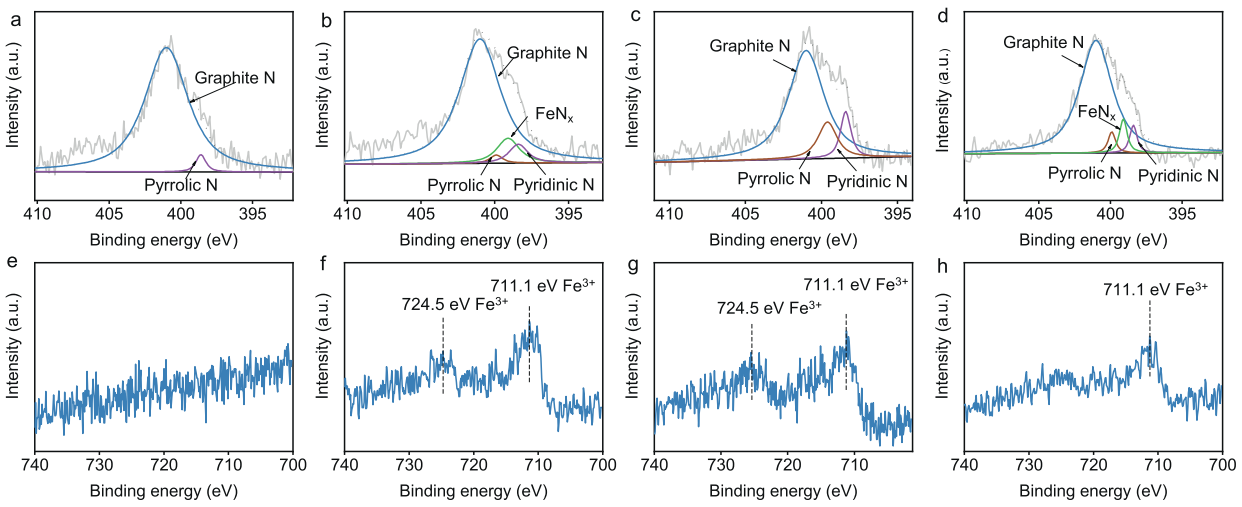

Fig. 1. High resolution N 1s and Fe 2p XPS spectra of 0%Fe-N/C (a, e), 5%Fe-N/C (b, f), 7.5%Fe-N/C (c, g), and 10%Fe-N/C (d, h).

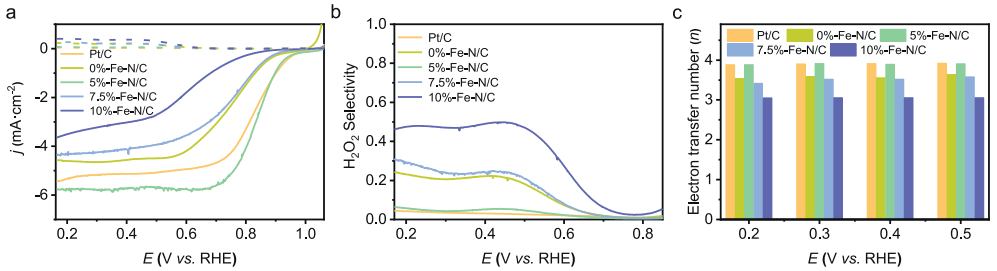

Fig. 2. ORR activity of the as-prepared Fe-N/C catalysts under 0.1 mol/L KOH condition. LSV curves in which the solid lines represent the disk current and the dotted lines represent the ring current (a), estimated H_2O_2 selectivity (b), and electron transfer number (c).

To measure the H_2O_2 accumulation level on catalyst surface, a biased potential was applied on platinum ring and the H_2O_2 oxidation current was collected. As shown in Fig. 2a, 5%Fe-N/C showed a comparable platinum ring current to that of Pt/C. The ring current density of 10%Fe-N/C was about 0.40 mA/cm^2 (Fig. 2a, Table S5), which was the highest. H_2O_2 selectivity calculation also validated the above results (Fig. 2b). The estimated electron transfer number (n) of 0%Fe-N/C, 7.5%Fe-N/C, and 10%Fe-N/C was at about 3.6, 3.5, and 3.0 in the range of 0.2–0.5 V, respectively (Fig. 2c). In comparison, the n value of 5%Fe-N/C was close to that of Pt/C, which were all near at 4.00, certificating an excellent selectivity of four-electron pathway. The above results clearly indicated that adding suitable amount of iron into tea leaves were beneficial for the four-electron ORR activity improvement while over dosage of iron would possibly alter catalyst structure and cause performance deterioration.

Considering the highest ORR activity of 5%Fe-N/C, additional electrochemical tests were conducted to evaluate its stability. The CV curve of 5%Fe-N/C in O_2 saturated 0.1 mol/L KOH solution showed a clear reduction peak at about 0.76 V; however, there was no peak in N_2 saturated solution (Fig. 3a), which again proved the ORR occurrence on this catalyst [37]. To assess the stability of 5%Fe-N/C, the LSV curves before and after 3000 cycles of CV tests were collected. As shown in Fig. 3b and Table S6 (Supporting information), only a slight decline (*i.e.*, 5.4%) of limiting current density, from 5.75 mA/cm^2 to 5.44 mA/cm^2, was observed on 5%Fe-N/C after stability tests. Whereas, a 7.5% dropped current intensity (decline from 5.44 mA/cm^2 to 5.03 mA/cm^2) was occurred on Pt/C. Moreover, the onset potential of 5%Fe-N/C changed little after 3000 cycles of CV tests (from 0.93 V to 0.92 V). In comparison, the onset potential of Pt/C declined from 0.93 V to 0.88 V. The half-wave potential also exhibited the similar trend. These results indicated that 5%Fe-N/C might perform a good stability under the long run.

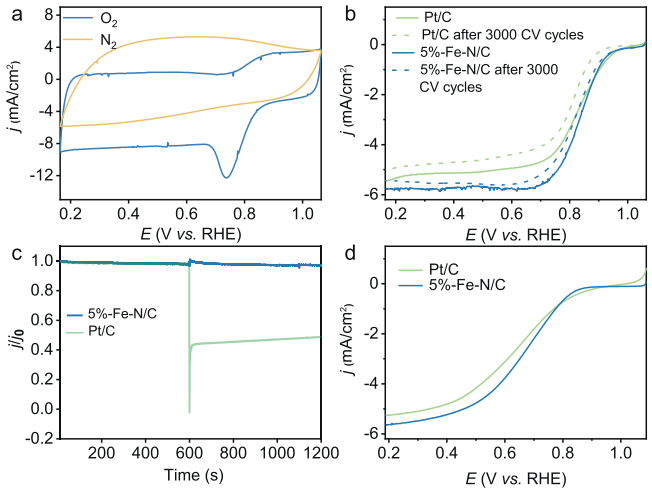

Fig. 3. The electrochemical stability of 5%Fe-N/C catalyst. CV curves of catalyst in 0.1 mol/L KOH electrolyte under O_2 or N_2 saturated condition without rotation (a), LSV curves of materials before and after 3000 CV cycles under oxygen-saturated electrolyte in 0.1 mol/L KOH (b), *i-t* curves of Pt/C and 5%Fe-N/C during 0.5 mol/L methanol tolerant test with an applied potential of 0.514 V (*vs.* RHE), where *j* is the real-time current density and j_0 is the initial current density (c), ORR performance of catalysts in 0.1 mol/L PBS (pH 7.0) electrolyte (d).

Pt/C is well known of being poisoned by methanol [38], as a result, the ability to tolerate methanol is another crucial factor for a ORR catalyst [39]. Methanol with 0.5 mol/L concentration was dosed into electrolyte at about 600 s and the *i-t* current curve was recorded. Results showed that methanol caused a negligible influence on 5%Fe-N/C performance (Fig. 3c). However, a near 60% drop of current was observed on Pt/C after methanol addition.

Apart from in alkaline soultion, ORR activity of catalyst in netural soultion is also applicable in practice [8]. Therefore, the LSV curves of 5%Fe-N/C and Pt/C in O_2-saturated 0.1 mol/L PBS (pH 7.0) were collected (Fig. 3d and Table S7 in Supporting information). Both the onset and half wave potential of 5%Fe-N/C (0.82 V and 0.64 V) were close to those of Pt/C (0.84 V and 0.64 V). Besides, the limiting current density of 5%Fe-N/C (5.64 mA/cm^2) was even higher than Pt/C (5.28 mA/cm^2). In comparison with other Fe-N/C and biomass derived catalysts, the performance of our fabricated Fe-N/C exhibited an outstanding performance (Tables S8-S10 in Supporting information). The above results indicated that 5%Fe-N/C owns an excellent ORR activity in both alkaline and neutral electrolyte.

Due to the inefficiency of XPS on characterizing catalyst fine structure, the specific iron-nitrogen coordination was measured by X-ray adsorption near-edge structure (XANES) and extended X-ray adsorption fine structure (EXAFS) analysis. The Fe *K*-edge XANES curves in Fig. 4a indicates that the oxidation valence state of catalysts was different from Fe foil while similar to that of Fe_2O_3 and Fe_3O_4, implying an oxidation state of iron. Fourier-transformed (FT) is a broadly adopted information extraction method to obtain further information of EXAFS spectra. As shown in Fig. 4b and Fig. S8 (Supporting information), 5%Fe-N/C showed a peak at 1.41 Å while the peaks of 7.5%Fe-N/C and 10%Fe-N/C shifted to 1.47 Å and 1.56 Å, respectively. In relation to the Fe—*O* bond (1.47 Å) in Fe_2O_3 curve, the shift of 5%Fe-N/C and 10%Fe-N/C suggests that the Fe center was not merely coordinated with oxygen, and there may exist Fe-N_x species within these two catalysts [40]. The above result was consistent with the XPS analysis. The coordination number of Fe and the mean bond length in 5%Fe-N/C were 6.4 ± 1.2 Å and 1.99 ± 0.02 Å (Table S11 in Supporting information). According to the fitting data, we proposed that the Fe atoms may bond with two O atoms and four N atoms (FeN_4O_2), which was matched well with the four-electron ORR activate sites in other researches [4,17]. For 10%Fe-N/C, the Fe may coordinate with four N atoms (FeN_4), which allowed to carry out the two-electron ORR route [41].

Besides the catalytic site, iron addition might also affect the catalyst conductivity and charge transfer resistance. Herein, both EIS

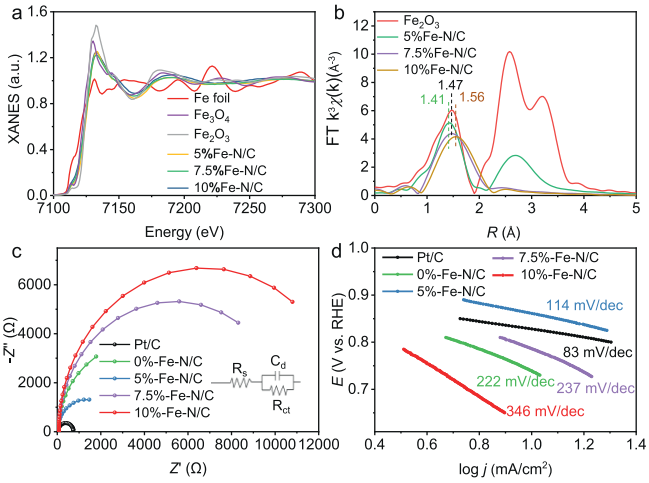

Fig. 4. Catalysts fine structure and electrochemical characterization. (a) Fe *K*-edge XANES spectra, (b) Fourier transform of the EXAFS spectra, (c) Tafel plots of the as-prepared catalysts, (d) EIS curves of the as-prepared catalysts.

and Tafel tests were performed. In Fig. 4c and Table S12 (Supporting information), as compared to other catalysts, 5%Fe-N/C showed the lowest charge-transfer resistance (R_{ct}, 2627 Ω), implying its superior conductivity, which is consistent with the results of Raman shift. Tafel slope of 5%Fe-N/C was 114 mV/dec, which was the nearest one to Pt/C among the other catalysts (Fig. 4d). Both Tafel and EIS tests showed a same trend that adding an appropriate amount of iron chloride can enhance the conductivity of the material, while over dosage will lead to a substantial increase of material resistance and the decrease of ORR kinetics. According to the XRD patterns (Fig. S3b), the Fe_3O_4 peak intensity of Fe-N/C catalyst was decreased with the rising of iron dosage. According to the previous work, the antiferromagnetic Fe_3O_4 was beneficial to increase the material conductivity [42,43]. The reduction of Fe_3O_4 while increase of non-ferromagnetic Fe_2O_3 might be the reason of material charge resistance increase [44].

By dosing appropriate amount of $FeCl_3$ into tea leaves precursor, the Fe-N/C catalyst with high four-electron ORR activity was sucessfully fabricated. The ORR activity of as-prepared 5%Fe-N/C catalyst were all comparable to that of commercial 20% Pt/C. In alkaline condition, 5%Fe-N/C owns a high ORR activity of onset potential (0.93 V), half-wave potential (0.84 V), and limiting current density (5.77 mA/cm^2), and in neutral media, the activity data are 0.82 V, 0.64 V and 5.64 mA/cm^2. Over-dosage of $FeCl_3$ would result in a declined four-electron selectivity. FeN_4O_2 might be the possible catalytic site for ORR. An appropriate amount of iron chloride not only facilitated catalytic site formation, but also enhanced the material conductivity and reaction kinetics.

Declaration of competing interest

The authors declare that they have no known competing financial interests or personal relationships that could have appeared to influence the work reported in this paper.

Acknowledgments

The authors wish to thank the National Natural Science Foundation of China (No. 51908172) for the support of this study.

Supplementary materials

Supplementary material associated with this article can be found, in the online version, at doi:10.1016/j.cclet.2022.02.041.

References

[1] X. Feng, Y. Bai, M. Liu, et al., Energy Environ. Sci. 14 (2021) 2036–2089.
[2] B. Wang, X. Cui, J. Huang, R. Cao, Q. Zhang, Chin. Chem. Lett. 29 (2018) 1757–1767.
[3] X. Hu, Y. Min, L.L. Ma, et al., Appl. Catal. B 268 (2020) 118405.
[4] K.A. Kuttiyiel, Y. Choi, K. Sasaki, et al., Nano Energy 29 (2016) 261–267.
[5] W.T. Wang, N. Batool, T.H. Zhang, et al., J. Mater. Chem. A 9 (2021) 3952–3960.
[6] M.A. Matin, J. Lee, G.W. Kim, et al., Appl. Catal. B 267 (2020) 118727.
[7] X. Chen, X. Zhen, H. Gong, et al., Chin. Chem. Lett. 30 (2019) 681–685.
[8] Z.Y. Yang, Y.X. Zhang, L. Jing, et al., J. Mater. Chem. A 2 (2014) 2623–2627.
[9] W. Wang, Q. Jia, S. Mukerjee, S. Chen, ACS Catal. 9 (2019) 10126–10141.
[10] L. Lin, Q. Zhu, A.W. Xu, J. Am. Chem. Soc. 136 (2014) 11027–11033.
[11] U.I. Kramm, M. Lefevre, N. Larouche, D. Schmeisser, J.P. Dodelet, J. Am. Chem. Soc. 136 (2014) 978–985.
[12] Y. Li, R. Hu, Z. Chen, et al., Nano Res. 14 (2020) 611–619.
[13] N. Ramaswamy, U. Tylus, Q. Jia, S. Mukerjee, J. Am. Chem. Soc. 135 (2013) 15443–15449.
[14] U.I. Kramm, I. Herrmann-Geppert, J. Behrends, et al., J. Am. Chem. Soc. 138 (2016) 635–640.
[15] Q. Lai, L. Zheng, Y. Liang, et al., ACS Catal. 7 (2017) 1655–1663.
[16] Y. Zhu, B. Zhang, X. Liu, D.W. Wang, D.S. Su, Angew. Chem. Int. Ed. 53 (2014) 10673–10677.
[17] A. Zitolo, V. Goellner, V. Armel, et al., Nature Mater. 14 (2015) 937–942.
[18] X. Wang, H. Zhang, H. Lin, et al., Nano Energy 25 (2016) 110–119.
[19] T. Liu, P. Zhao, X. Hua, et al., J. Mater. Chem. A 4 (2016) 11357–11364.
[20] Y. Shangguan, Y. Zhou, R. Zheng, et al., Chin. Chem. Lett. 32 (2021) 3450–3456.
[21] Z. Chen, R. Zheng, W. Wei, et al., Chen, Resour. Conserv. Recycl. 178 (2022) 106037.
[22] Z. Chen, R. Zheng, S. Li, et al., Chem. Eng. J. 431 (2022) 134304.
[23] Z. Chen, R. Zheng, S. Deng, et al., J. Mater. Chem. A 9 (2021) 25032–25041.
[24] X. Wang, J. Du, Q. Zhang, et al., Carbon 157 (2020) 614–621.
[25] H. Ejima, J.J. Richardson, L. Kang, et al., Science 341 (2013) 154–157.
[26] Y.H. Zhao, B.C. Huang, J. Jiang, W.J. Xia, R.C. Jin, Chemosphere 244 (2019) 125577.
[27] S. Wong, Y. Lee, N. Ngadi, I.M. Inuwa, N.B. Mohamed, Chin. J. Chem. Eng. 26 (2018) 1003–1011.
[28] H. Cai, H. Zou, J. Liu, et al., Bioresour. Technol. 268 (2018) 715–725.
[29] F. Zhu, S. Ma, T. Liu, X. Deng, J. Clean. Prod. 174 (2018) 184–190.
[30] Y. Liu, H. Feng, F. Luo, Carbon 161 (2020) 153–161.
[31] R. Song, Q. Wang, B. Mao, et al., Carbon 130 (2018) 164–169.
[32] G. Wu, K.L. More, C.M. Johnston, P. Zelenay, Science 332 (2011) 443–447.
[33] Y. Lou, J. Liu, M. Liu, F. Wang, ACS Catal. 10 (2020) 2443–2451.
[34] H. Ren, Y. Wang, Y. Yang, et al., ACS Catal. 7 (2017) 6485–6492.
[35] Z. Guo, Z. Xiao, G. Ren, et al., Nano Res. 9 (2016) 1244–1255.
[36] T. Shahwan, S. Abu Sirriah, M. Nairat, et al., Chem. Eng. J. 172 (2011) 258–266.
[37] R. Zhang, M. Tahir, S. Ding, et al., ACS Appl. Energy Mater. 3 (2019) 2323–2330.
[38] Q. Xiang, Y. Liu, X. Zou, et al., ACS Appl. Mater. Interfaces 10 (2018) 10842–10850.
[39] H. Zhao, Y. Zhang, L. Li, et al., Chin. Chem. Lett. 32 (2021) 140–145.
[40] F. Xiao, G.L. Xu, C.J. Sun, et al., Nano Energy 61 (2019) 60–68.
[41] J.H. Zagal, M.T.M. Koper, Angew. Chem. Int. Ed. 55 (2016) 14510–14521.
[42] W.J. Yin, S.H. Wei, C. Ban, et al., Phys. Chem. Lett. 2 (2011) 2853–2858.
[43] A. Radoń, P. Włodarczyk, A. Drygała, D. Łukowiec, Appl. Surf. Sci. 474 (2019) 66–77.
[44] Y. Tian, X. Hu, Y. Wang, C. Li, X. Wu, A.C.S. Sustain, Chem. Eng. 7 (2019) 9211–9219.